RSC Advances

ROYAL SOCIETY OF CHEMISTRY

www.rsc.org/advances

Flammability properties and electromagnetic interference shielding of PVC/graphene composites containing Fe_3O_4 nanoparticles

Kun Yao [a, b], Jiang Gong [a, b], Nana Tian [a], Yichao Lin [a, b], Xin Wen [a], Zhiwei Jiang [a,*], Hui Na [c] and Tao Tang [a,*]

Received (in XXX, XXX) Xth XXXXXXXXX 20XX, Accepted Xth XXXXXXXXX 20XX
DOI: 10.1039/b000000x

Effects of the combined graphene/Fe_3O_4 nanoparticles on the flame retardancy and smoke suppression of PVC were studied. The dispersion state of graphene in PVC matrix was improved with the help of Fe_3O_4 nanoparticles. As a result, the peak values of heat release rate and smoke production rate measured by cone calorimeter were obviously decreased in the PVC/graphene/Fe_3O_4 composites. According to the results from TGA tests and structural characterization of residual char, the improved flame retardancy was partially attributed to the formation of a network-like structure due to the good dispersion state of graphene in PVC matrix, and partially to the carbonization of degradation products of PVC catalyzed by Fe_3O_4 nanoparticles. In addition, ternary PVC composites showed higher mechanical properties than pure PVC. More importantly, the resulting material possessed both electrical and magnetic properties. As a result, the ternary composites showed favorable electromagnetic shielding efficiency in the x-band frequency region (8-12 GHz), due to the formation of conducting interconnected graphene-based networks in the insulating PVC matrix and the magnetic properties.

1 Introduction

Commercial polyvinyl chloride (PVC) is a uniquely versatile polymer with the third largest tonnage after polyethylene and polypropylene.[1-2] Owing to its high mechanical strength, high corrosion resistance and relatively low cost, PVC has been extensively used for pipes, doors, windows, *etc*.[3] However, for applications where flexible or semi-rigid PVC is required, certain organic plasticizers such as dioctylphthalate (DOP) are incorporated at varying levels. The presence of a plasticizer has dramatic effects on not only the mechanical properties, but also the flammability and smoke production when PVC decomposes thermally.[4-5]

It has been proved that most metal compounds, in particular, transition metal compounds (such as copper, molybdenum and iron compounds) are the most effective smoke retarders.[6-8] Two mechanisms at the molecular level, 'reductive coupling' and 'Lewis acid', are applied to explain the crosslinking reaction between PVC chains.[6, 9] Some previous researches on the flame retardancy, smoke emission and thermal degradation of PVC with transition metal oxides has been reported,[6, 10-11] however, mechanical properties and other properties are not mentioned. It is well known that layered nanomaterials can also play an important role in the flame retardancy of polymer nanocomposites.[12-13] Wang *et al.* investigated the effect of hydrotalcite on the mechanical properties and flame retardancy of PVC. The results showed that the deterioration of the mechanical properties was negligible, and PVC composites exhibited good flame retardancy with UL94 V-0 as well as good smoke suppression.[11] Beyer found that the presence of hectorite and modified montmorillonite reduced the peak of heat release rates and lower smoke production rate of PVC compared to the case without filler.[14] The influence of montmorillonite modified by silane coupling agents (*e.g.*, c-aminopropyltriethoxysilane) and copper compounds (cupric sulfate) on the smoke suppression and flame retardancy of PVC was also tested by Yang *et al.*[15] Their experimental results showed that OMMT containing Cu^{2+} promoted the early crosslinking of PVC chains and increased the char residue.

Graphene has become of great interests, both from a fundamental research and for their potential applications.[16-17] As a nanofiller, it may be preferred over other conventional nanofillers (Na-MMT, LDH, CNT, CNF, EG, *etc.*) due to its high surface area, aspect ratio, tensile strength, flexibility, flame retardancy and electrical conductivity.[18-22] These intrinsic properties of graphene have generated enormous interests for its possible performance in polymer nanocomposites. However, to effectively endow a matrix polymer with such high-performance, homogeneous dispersion of nanofillers in polymer matrix must be achieved.[23] Many studies on graphene dispersion have been flourished in the last half decade, including non-covalent and covalent modifications.[24] Non-covalent functionalization of graphene sheets was achieved by wrapping and adsorbing polymers under the binding force of π–π interactions.[25-26] Stable dispersions of graphene in organic solvents or water media were obtained by using polyelectrolytes, surfactants and organic molecules, such as phenyl isocyanate and porphyrin.[27-28] Covalent modification is chemically functionalized through directly introducing functional groups or polymer chains onto the graphene surface by 'grafting from' or 'grafting to' method.[29-30] However, these methods seemed not fit for mass production. As far as we known, there are few references about PVC/graphene nanocomposites, none of them involved other nanoparticles at the same time.[25, 29, 31, 32]

In this work, we demonstrated that the addition of Fe_3O_4 nanoparticles could improve the dispersion state of graphene (GE) in PVC matrix. Compared to PVC/GE or PVC/Fe_3O_4,

PVC/GE/Fe_3O_4 ternary composites showed excellent flame retardancy, smoke suppression and superior mechanical properties. Owing to the inherent electrical conductivity of graphene and the magnetic properties of Fe_3O_4 nanoparticles, the final PVC/GE/Fe_3O_4 composites presented not only superparamagnetism but also electrical conductivity. What's more, it performed high electromagnetic shielding efficiency.

2 Experimental Section

2.1 Materials

Polyvinyl chloride (PVC) was purchased from Aldrich (M_w = 80000 g/mol). Graphite powder, di-n-octylo-phthalate (DOP) and dibutyltin dilaurate were purchased from Sinopharm Chemical Reagent Beijing Co., Ltd. 98% H_2SO_4, 30% H_2O_2, $KMnO_4$, ferric chloride, ferrous sulfate and ammonium hydroxide (25% NH_3), were purchased from Shanghai Zhenxin Chemical Company. Oleic acid (OA) was purchased from Aldrich.

2.2 Synthesis of Graphene

Graphene oxide was prepared with improved Hummers' method.[33] In a typical process, a 9:1 mixture of concentrated H_2SO_4/H_3PO_4 (360:40 mL) was added to a mixture of graphite flakes (3.0 g, 1 wt equiv) and $KMnO_4$ (18.0 g, 6 wt equiv). The reaction was then heated to 50 °C and stirred for 12 h. The reaction was cooled to room temperature and poured onto ice (400 mL) with 30% H_2O_2 (3 mL). After multiple-wash process, the solid obtained was vacuum-dried at room temperature. For thermal exfoliation, the dried graphite oxide is charged into a quartz tube and purged with argon. Rapid heating (>2000 °C /min) to 1050 °C splits the graphite oxide into individual sheets through evolution of CO_2.[34]

2.3 Synthesis of Fe_3O_4 Nanoparticles

To synthesize Fe_3O_4 nanoparticles, we followed the standard chemical coprecipitation route. Ferrous sulfate (4 g) and ferric chloride (11 g) were added to deionized water (200 mL) and heated to 90 °C under argon in a three-necked, round-bottomed flask, while magnetically stirring the mixture.[35] Ammonium hydroxide solution (25 mL, 28%) was injected into the solution. Oleic acid (6 g) was added soon, it was heated for 1 h, and the entire solution was neutralized with HCl. Fe_3O_4 nanoparticles were magnetically decanted and washed three times with deionized water, and then dissolved in hexane removing the un-dissolved part. As a final step, the hexane was evaporated, leaving the dry nanoparticulate residue in powder form.

2.4 Preparation of PVCxGyFe composites

Polyvinyl chloride (PVC) was mixed with 50 wt% DOP, 5 wt% dibutyltin dilaurate, graphene and Fe_3O_4 nanoparticle compounds in a Brabender mixer at 80 rpm and 145 °C for 8 min. The content of Fe_3O_4 (5 wt%) was selected according to previous reports.[36] The resultant samples were designated as PVCxGyFe. Here G and Fe denote graphene and Fe_3O_4 nanoparticles, respectively; and x and y denotes the weight percentage of graphene and Fe_3O_4, respectively. For example, PVC3G5Fe means that the sample contains 3 wt% graphene and 5 wt% Fe_3O_4 nanoparticles.

2.5 Characterization

Morphologies of the graphene and Fe_3O_4 nanoparticles were observed by means of transmission electron microscope (TEM, JEOL1011) at 100 kV accelerating voltage. The surface element compositions of graphene and Fe_3O_4 nanoparticles were characterized by means of X-ray photoelectron spectroscopy (XPS) carried out on a VG ESCALAB MK II spectrometer using an Al Kα exciting radiation from an X-ray source operated at 10.0 kV and 10 mA. The phase structure was analyzed by X-ray powder diffraction (XRD) using a D8 advance X-ray diffractometer with Cu Kα radiation operating at 40 kV and 200 mA.

The dispersion was observed by TEM. Ultrathin sections were cryogenically cut using a Leica Ultracut and a glass knife at -80 °C, the samples were collected on carbon-coated copper TEM grids. The surface element of graphene was analyzed using field-emission scanning electron microscope (SEM, XL30ESEM–FEG) with an energy dispersive X-ray spectrometer (EDX, Genesis 2000).

Cone calorimeter tests were performed according to ISO5660 standard at a heat flux 50 kW/m^2. Exhaust flow rate was 24 L/s and the spark was continuous until the sample ignited. The samples for the test of cone calorimeter were hot pressed by compression molding at 160 °C with the size of (100×100×3) mm^3 square plaques. After cone calorimeter test, the residues were observed by field-emission scanning electron microscope (SEM, XL30ESEM–FEG). The limiting oxygen index (LOI) values were measured on an HC-2C oxygen index meter (Jingning Analysis Instrument Company, China) with sheet dimensions of (130×6.5×3) mm^3 according to ISO4589-1984. The vertical burning tests were tested according to the UL-94 test standard (ASTM D 3801) with the test specimen was (130×13×3) mm^3. TGA was carried out with a Q600 thermal analyzer (TA Co., New Castle, USA) from ambient temperature to 650 °C at a heating rate of 10 °C/min under nitrogen with a flowing rate of 100 mL/min. Mechanical properties were measured on an Instron 1121 at an extension speed of 20 mm/min. At least five tests were conducted for each sample, from which the mean values and standard deviations were derived.

Magnetic susceptibility data was measured with a Quantum Design MPMS XL-7 SQUID magnetometer at room temperature (300 K). The electrical conductivity of composites was also measured with a four-probe technique under ambient conditions. The EMI shielding effectiveness and complex (relative) permittivity data of PVC composites were measured with the slabs of dimension of (22.8×10.2×1.8) mm^3 to fit waveguide sample holder using a PNA-X Network Analyzer (N5244a) in 8.2-12.4 GHz (X band).

3 Results and discussion

3.1 Characterization of graphene and Fe_3O_4 nanoparticles

The obtained graphene were fully analyzed by TEM, XRD and XPS measurements. Fig. 1 displays the TEM images of graphene and Fe_3O_4 nanoparticles assisted by ultrasonic in THF. The flake dimension is 0.7-1.4 μm, and clearly most of them are single or two layers. It can be observed that the Fe_3O_4 particles are nearly spherical with the diameter of about 6-11 nm. Fig. 2 exhibits the

XRD patterns of graphene and Fe_3O_4 nanoparticles. The appearance of narrow 25.8 ° (002) diffraction peak indicated the high degree of graphitization (Fig. 2a). The diffraction peaks of Fe_3O_4 nanoparticles, *i.e.* 30.2° (220), 35.5° (311), 43.2° (400), 54.1° (422), 57.1° (511) and 62.7° (440) appeared (Fig. 2b), but it is very difficult to distinguish Fe_3O_4 and γ-Fe_2O_3 only by XRD measurements. So XPS was used to further characterize the particles. The spectrum of Fe 2p of nanoparticles (Fig. 3a) indicated the existence of doublet Fe $2p_{3/2}$ and Fe $2p_{1/2}$ with binding energies of about 711 eV and 724 eV, respectively. The absence of the satellite peak situated at about 719 eV, which was a major characteristic of Fe^{3+} in γ-Fe_2O_3, clearly suggested the existence of Fe_3O_4.[37] The reduction of graphene was also characterized using XPS. Figure 3b shows the XPS spectra in the C1s and O1s region of graphene after reduction. After reduction (Fig. 3b), the peaks centered at 284.5 and 288.8 eV were observed, which corresponded to C=C/C–C in aromatic rings, COOH, and C(O)O groups, respectively. The intensities of all C1s peaks of the carbon binding to oxygen were quite low, revealing that most oxygen containing functional groups were removed during reducing reaction.

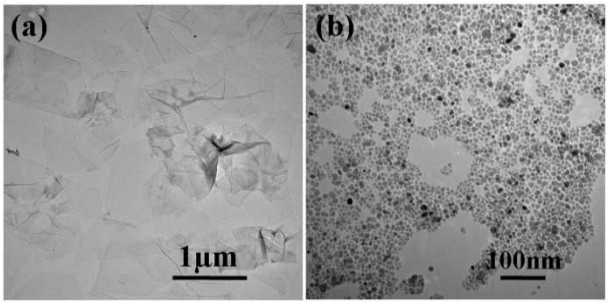

Fig. 1 TEM image of graphene and Fe_3O_4 nanoparticles. (a) graphene (b) Fe_3O_4 nanoparticles.

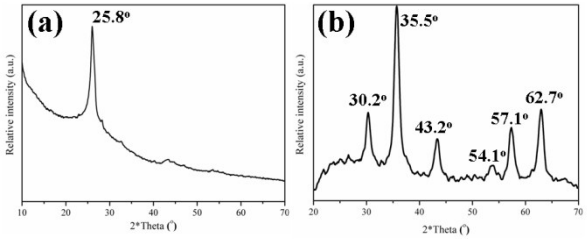

Fig. 2 XRD patterns of graphene and Fe_3O_4 nanoparticles. (a) graphene (b) Fe_3O_4 nanoparticles.

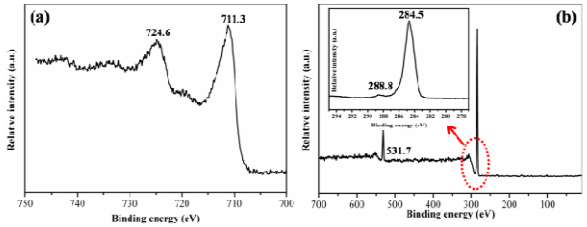

Fig. 3 The XPS spectra in the C1s region of graphene and Fe 2p of nanoparticles: (a) Fe_3O_4 nanoparticles; (b) graphene

3.2 Dispersion States of Graphene and Fe_3O_4 nanoparticles in PVC Matrix

The properties of polymer nanocomposites strongly depend on the dispersed state and exfoliated state of graphene platelets with high aspect ratios in polymer matrix. TEM observation was carried out to compare the morphologies of PVC binary composites with those of PVC ternary composites. As shown in Fig. 4a, Fe_3O_4 nanoparticles are dispersed as aggregates with the size of 20-80 nm in the PVC5Fe sample. Numerous agglomerated particles of graphene platelets were detected in the PVC5G sample (Fig. 4b), which result from the polarity mismatch between graphene and PVC matrix. In contrast, the dispersed state of graphene in PVC matrix with 5 wt% Fe_3O_4 was totally different (Fig. 4c). The graphene was well dispersed in PVC matrix, and uncorrelated nanosheets were clearly visible, confirming the uniform dispersion with few agglomeration. It has been reported hybrid ternary systems with two nanoscale materials have shown very promising in enhancing the dispersion of nanoparticles.[38] Kong *et al.* revealed interactions between alumina and silica sol and suggested a nanoparticle-haloing model of the silica nanoparticles scattered around the large alumina particles. They found reduced sedimentation of alumina particles due to the presence of silica nanoparticles.[38] In this work, what is the driving force to make the graphene exfoliated easily in the presence of Fe_3O_4 nanoparticles? It is speculated that the graphene sheets were insulated by Fe_3O_4 nanoparticles, reducing the interaction between graphene. Owing to the Fe_3O_4 covered by oleic acid ligand, the Fe_3O_4 nanoparticles were easily attached to the graphene containing residual oxygen groups *via* a ligand exchange process during mixing procedure. Thus the presence of Fe_3O_4 nanoparticles weakened the interaction between graphene and increases the interaction between polymer and graphene. To prove this idea, we made a model experiment, where graphene and Fe_3O_4 nanoparticles were mixed in THF via ultrasound for 10 min, and then the TEM observations are done. Very obviously, the Fe_3O_4 nanoparticles indeed deposited on the surface of graphene as deemed (Fig. 4d). In addition, as shown in Fig. 4e, some white particles can be detected on the surface of graphene in the fractured surface of PVC5G5Fe nanocomposites. The main element of them is confirmed to be Fe from EDX map in the magnified SEM image (Fig. 4f), showing that Fe_3O_4 nanoparticles existed on the surface of graphene. Therefore, the interfacial interaction between PVC and graphene will be improved due to the presence of oleic acid on the Fe_3O_4 nanoparticles. It should be mentioned that due to the longitudinal section of graphene in PVC matrix, Fe_3O_4 nanoparticles locating on graphene surface are not easy to be detected in the ultrathin section sample. The use of co-dispersed hybrid system is expected to improve the flame retardancy, mechanical properties and electromagnetic shielding performance.

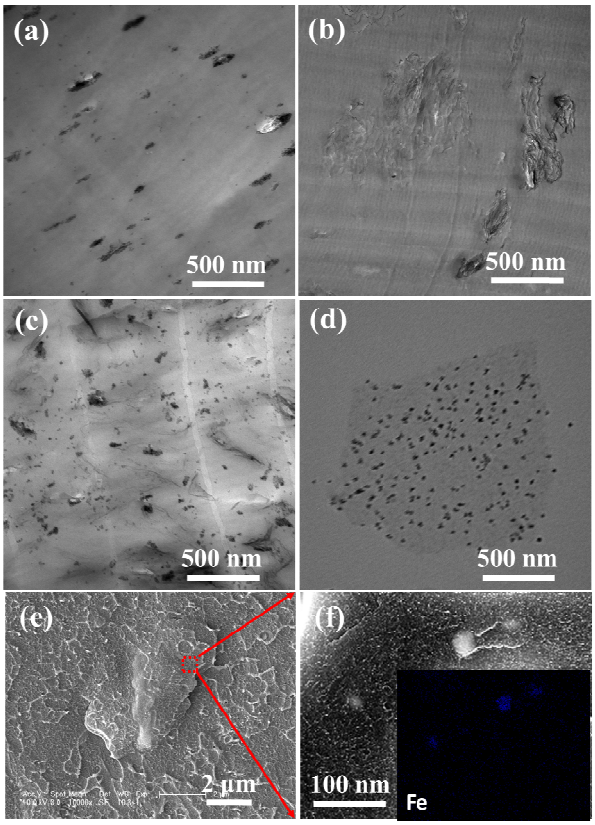

Fig. 4 TEM micrograph of PVC and PVC nanocomposites. (a) PVC5Fe (b) PVC5G (c) PVC5G5Fe (d) model experiment with Fe_3O_4 nanoparticles and graphene (e) SEM image of PVC5G5Fe (f) SEM image and EDX map of PVC5G5Fe

3.3 Flammability properties

The influence of the combined graphene/Fe_3O_4 nanoparticles on the flame retardancy of PVC matrix was investigated by means of cone calorimetry. Cone calorimetry is one of the most effective medium-sized polymer fire behavior tests. It provides comprehensive insights into fire risk *via* parameters such as the heat release rate (HRR), the total heat release (THR), the smoke production rate (SPR) and total smoke produced (TSP).[39] Table 1 summarise the results of cone calorimeter tests at 50 kW/m^2 for PVC and its composites. Fig. 5 shows the HRR plots of PVC and its composites. Neat PVC burnt very fast after ignition, and a sharp HRR peak appeared with a peak value of HRR (PHRR) as high as 289.4 kW/m^2. The PHRR in the HRR plot of binary PVC3G or PVC5G composites decreased slightly compared to that of neat PVC, indicating that the flammability of PVC was not influenced strongly by adding graphene alone in the matrix. Similarly, the PHRR of binary PVC5Fe composite (211.5 kW/m^2) reduced by 27% compared to that of neat PVC, suggesting that the addition of graphene or Fe_3O_4 nanoparticles alone could not effectively improve the flame retardancy of PVC as well. However, when the combination of graphene and Fe_3O_4 nanoparticles was applied, the PHRR from the HRR plots of the ternary PVCxGyFe composites showed an obvious reduction compared with that of the binary PVC5G or PVC5Fe composite, for example, PHRR =150.8 kW/m^2 for PVC3G5Fe, reduced by 48% compared to that of neat PVC. It was noteworthy that the HRR of ternary PVC5G5Fe composite showed the lowest peak value (PHRR = 112.0 kW/m^2, reduced by 61% compared to that of neat PVC). Table 1 also presents the THR data for PVC and its composites. Compared to neat PVC, the THR of binary PVC5G and PVC5Fe composites was reduced by 2% and 31%, respectively. Notably, the THR of ternary PVC5G5Fe composite further decreased to 20.0 MJ/m^2, the value of which was reduced by 51% compared to that of neat PVC. The lower THR value means that a part of PVC was converted into residual char without complete combustion. As we know, if the char results from the degradation products of polymer itself when exposed to fire conditions, the amount of flammable volatiles evolved will be reduced, and the flame retardancy of the polymer will be improved. As expected, the yield of the residual chars from the cone calorimeter tests was obviously increased in the cases of ternary composites (Table 1). This means that there are relatively fewer pyrolytic flammable gases to volatilize during combustion in the case of the ternary PVC5G5Fe composite. To further investigate the effect of the combined graphene/Fe_3O_4 nanoparticles on the flame retardancy of PVC matrix, LOI and UL-94 tests were carried out. As listed in Table 1, the LOI values slightly increased with the addition of nanofillers from 27.4 for neat PVC to 29.6 corresponding to ternary PVC5G5Fe composite. The UL-94 grade was upgraded from V1 grade to V0 grade in the cases of binary PVC5Fe and ternary composites. Clearly the presence of Fe_3O_4 nanoparticles was more efficient to improve the flame retardancy of PVC comparing with the case containing graphene (Table 1).

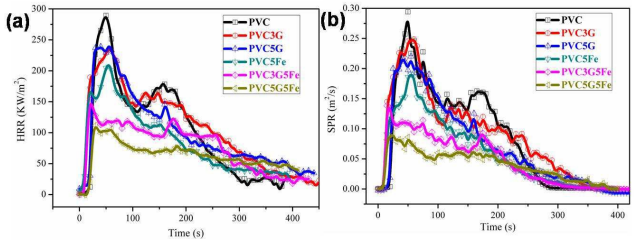

Fig. 5 (a) The heat release rate (HRR) and (b) the smoke production rate (SPR) for PVC and its composites

Table 1. Summary of the cone calorimetric (at 50 kW/m^2), LOI and UL-94 results for PVC and its composites.

Samples	Residual char (wt %)	PHRR (kW/m^2)	THR (MJ/m^2)	PSPR（m^2/s）	TSP (m^2/kg)	LOI	UL-94
PVC	8.1	289.4	40.6	0.294	896.4	27.4	V1
PVC3G	8.4	242. 6	40.1	0.249	879.7	27.6	V1
PVC5G	8.8	237.4	39.9	0.220	810.2	28.0	V1
PVC5Fe	15.2	211. 6	28.1	0.191	617.5	28.3	V0
PVC3G5Fe	16.0	150.8	24.2	0.112	536.7	29.0	V0
PVC5G5Fe	16.3	112.0	20.0	0.092	443.3	29.6	V0

As well known, smoke suppression is often more important in the flame retardancy of PVC. It can be clearly seen from Fig. 5b that pure PVC burns with PSPR as high as 0.294 m^2/s. The addition of graphene (PVC5G) or Fe_3O_4 (PVC5Fe) changed slightly reduced that the PSPR of PVC, however, the ternary PVCxGyFe composite leads to much reduction in PSPR, and the ternary PVC5G5Fe composite exhibits the lowest PSPR value (0.092 m^2/s), which is reduced by 69% compared to that of PVC. Furthermore, a similar change trend was observed in TSP behavior. Compare to PVC, PVC5G5Fe shows a decrease of TSP by 50% from 896.4 m^2/kg of PVC to 443.3 m^2/kg.

The TGA curves of PVC and PVC nanocomposites are presented in Fig. 6 respectively. The temperatures of 10 wt % mass loss, $T_{10\%}$ (^{o}C), the temperatures of maximum mass loss, $T_{max\%}$ (^{o}C) and the residual mass (M_{600}, wt%) at 600 ^{o}C are summarized in Table 2. PVC and its nanocomposites reveal two stages of decomposition. The first stage may be attributed to PVC degradation and its additives. The mass loss during PVC degradation includes sequential loss of hydrogen chloride accompanied by the generation of polyene sequences. The $T_{10\%}$ of PVC is 273.6 ^{o}C with a T_{max} decomposition temperature at 315.8 ^{o}C and presents a residual mass of 6.8 wt% at 600 ^{o}C. The $T_{10\%}$ of PVC/graphene compositex is almost the same as that of PVC. However, the presence of Fe_3O_4 nanoparticles play an important role of accelerating the decomposition to release hydrogen chloride. The $T_{10\%}$ in the case of PVC5Fe is decreased by about 10 ^{o}C and the T_{max} is 44 ^{o}C lower than that of unfilled PVC. Nevertheless the mass loss during this degradation stage is reduced compared to PVC (Table 2), indicating that the char results from the degradation products of polymer with the help of Fe_3O_4 nanoparticles.

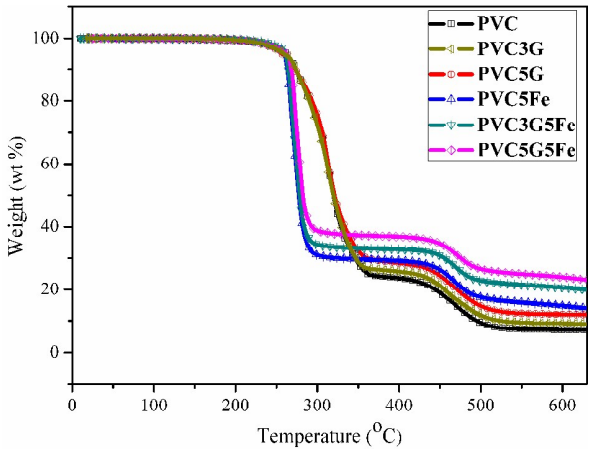

Fig. 6 TGA curves of PVC and PVC composites under N_2 atmosphere at 10 ^{o}C min^{-1}

Table 2. Thermal decomposition properties of PVC and its nanocomposites under nitrogen

Samples	$T_{10wt\%}$ (^{o}C)	$T_{max\ wt\%}$ (^{o}C)	M_{600} (wt %)
PVC	273.6	315.8	6.8
PVC3G	273.7	317.6	9.0
PVC5G	273.0	318.5	11.9
PVC5Fe	263.1	271.3	13.7
PVC3G5Fe	264.6	274.2	19.6
PVC5G5Fe	268.0	279.8	22.6

Lewis acid mechanism for smoke suppression in PVC using metal-containing compounds has been proposed in many previous reports. The final conclusion for this mechanism is that

all the iron compounds promote early crosslinking of PVC during decomposition to increase char formation. So the presence of iron-containing compounds can greatly reduce smoke formation during the pyrolysis or combustion of PVC. $FeCl_2$ and $FeCl_3$, which are *in situ* formed along with the thermal decomposition of PVC, act as an effective catalyst for the ionic dehydrochlorination of PVC due to their strong Lewis acidity. Dehydrochlorination of PVC in the presence of $FeCl_2$ and $FeCl_3$ occurs with a formation of trans-polyene structures followed by intermolecular cyclization.[40-41] In addition, phthalic acid has been identified as a key component in smoke formation during the combustion of plasticized PVC. It was established by Carty *et al.* that DOP plasticizer being an ester is readily decomposed into phthalic acid by hydrogen chloride produced from PVC and eventually forming large amount of smoke. The hydrogen chloride is "used up" in the presence of Fe_3O_4 nanoparticles and consequently the smoke is considerably lower than that of PVC without Fe_3O_4 nanoparticles.[4]

What's more, according to the TGA analysis, it is observed that PVC5G5Fe nanocomposite reveals $T_{10\%}$ temperatures 4.5 ^{o}C higher and T_{max} 8 ^{o}C higher compared to PVC5Fe. The positive effect of improved particle dispersion on the quality of protective layers of residue was reported by Kashiwagi et al. for carbon nanotubes.[42] Schartel *et al.* have concluded for polypropylene/carbon materials that a closed residual surface is necessary at the macroscopic as well as the microscopic scale to obtain effective flame retardancy by nanocomposites.[43] The graphene in PVC3G and PVC5G showed poor dispersion, as a result, the residue did not cover the sample entirely.

In the PVC5G5Fe nanocomposites, we speculate that the combination of graphene/Fe_3O_4 probably promotes the carbonization of the degradation products of PVC into char, which shows high resistance to oxidation. According to the above results, a conclusion could be drawn that the combination of graphene/Fe_3O_4 showed an effective effect on promoting the flame retardancy of PVC, because it significantly reduced the HRR, THR, SPR and TSP, and improved the yields of residual chars of PVC during combustion.

To investigate the effect of graphene with Fe_3O_4 nanoparticles on improving the flame retardancy of PVC, the yield and morphology of the residual chars after the cone calorimeter tests were analyzed, which was helpful to clarify the combustion behavior of the polymer materials. Fig. 7 present photographs of the residual chars from PVC and its composites after cone calorimeter tests. There is little amount of char residue with very loose state for neat PVC. Similar results were found in the cases containing 3 and 5 wt % graphene alone. In the previous study, it was found that the main degradation products of PVC were benzene and naphthalene, which could be catalyzed into char by Fe_2O_3.[40] In the case of the binary PVC5Fe composite, there is a carbon block left with similar shape as original PVC (about 4.9 wt%), because Fe_3O_4 nanoparticles could significantly accelerate the carbonization on the surface of PVC (Fig. 7). Very interesting, the combination of graphene/Fe_3O_4, especially PVC5G5Fe showed dense char surface. The volume of the residual char was large. It is assumed that the residual char combined with the well dispersed graphene plays a role of compact physical barrier, which prevents the degradation products (or oxygen) from the diffusion out of the surface (or entering the inside of sample).

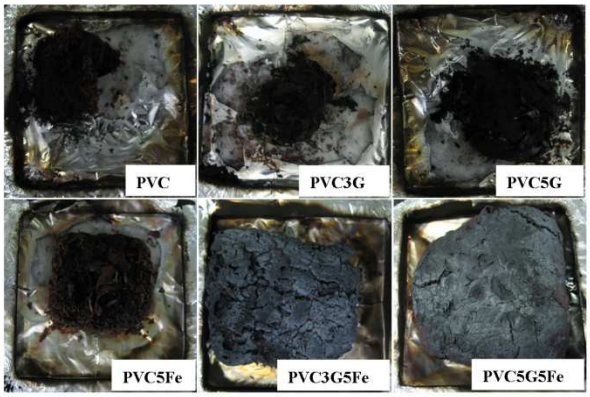

Fig. 7 Photographs of the residual chars after the cone calorimeter tests

Fig. 8 displays SEM images of the surface residual char for different samples after cone calorimeter tests. As for pure PVC, a large number of holes can be seen due to the release of hydrogen chloride and benzene, *etc* (Fig. 8a). While a lot of graphene aggregates is observed in the residual char from the binary PVC5G composite (Fig. 8c). Comparatively, octahedral Fe_3O_4 particles are exposed onto the surface of the char from the binary PVC5Fe (Fig. 8b). This phenomenon has been discussed in our previous study.[37] In PVC5G5Fe sample, both graphene and carbon residue can be effectively combined into a compact and continuous whole (Fig. 8d), which is very helpful for flame retardancy and smoke suppression.

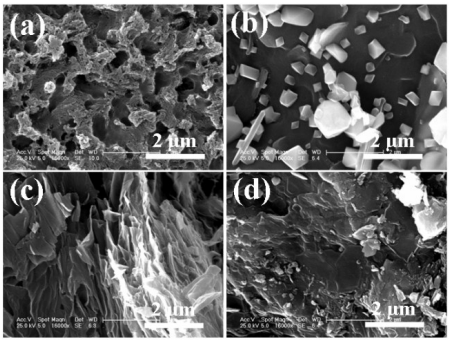

Fig. 8 SEM images of char residues for PVC composites (a) PVC (b) PVC5Fe (c) PVC5G (d) PVC5G5Fe

3.4 Mechanical properties

Generally, the well-dispersed state of fillers in polymer matrices is the key factor in order to prepare polymer composites with high mechanical properties. Otherwise, the addition of fillers leads to the formation of some defects; as a result, the mechanical properties of the composite will be deteriorated. Fig. 9 shows stress-strain curves of PVC and its nanocomposites. The tensile properties of the composites are given in Table 3. Compared to PVC, the addition of graphene alone in the PVC matrix does not show any obvious improvement in the Young's modulus, tensile strength and ultimate strain, which is attributed to poor dispersion states of graphene in PVC matrix (Fig. 4b). Although the addition of Fe_3O_4 nanoparticles enhance the modulus of matrix, the tensile strength is not improved, and the elongation at break is decreased. This may be the limitation of zero-dimensional structure of

nanoparticles. Very strikingly, the simultaneous presence of graphene and Fe_3O_4 nanoparticles show a remarkable reinforcing effect. As shown in Fig. 9 and Table 3, the modulus and tensile strength increased with the content of graphene, for example, up to 20.8% increase in tensile strength and up to a 73.7% increase in Young's modulus at the loading of 5 wt% graphene and 5 wt% Fe_3O_4 nanoparticles. The good dispersion of graphene in PVC matrix and the improved interaction between the oleic acid from Fe_3O_4 nanoparticles and matrix contribute to the mechanical improvement. Reasonably, the elongation at break of the composites reduced, comparing with PVC. Similar results were also reported by other coworkers.[32, 43] The reason may be attributed to a large aspect ratio and the well dispersion states of graphene, which restricts the movement of the polymer chains. The presence of graphene in the PVC matrix offers resistance to the segmental movement of polymer chains upon application of tensile stress, which led to enhancement in modulus. It is worth mentioning that the method for improving flame retardancy of polymeric materials by adding fillers without sacrificing mechanical properties simultaneously is very attractive to academic and industrial communities.

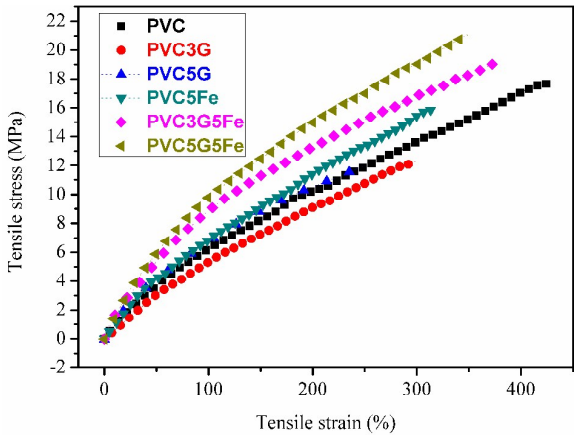

Fig. 9 Representative stress-strain behavior for PVCxGyFe nanocomposites

Table 3. Mechanical properties of composites.

Samples	Yong's Modulus (MPa)	Tensile strength (MPa)	Elongation at break (%)
PVC	8.89±0.8	17.8±0.1	425.3±22.3
PVC3G	5.89±1.1	12.3±1.3	299.8±40.8
PVC5G	11.67±1.3	11.9±1.1	248.7±39.6
PVC5Fe	10.58±0.7	15.8±0.4	315.6±30.0
PVC3G5Fe	13.82±0.5	19.2±1.0	377.5±25.9
PVC5G5Fe	15.44±0.8	21.5±1.2	349.1±23.5

3.5 Magnetic Properties

The magnetic properties of composites were further investigated. The magnetic hysteresis loops for Fe_3O_4 nanoparticles and the corresponding nanocomposites are shown in Fig. 10. The magnetization hysteresis loops are S-like, and neither remanence nor coericivity is observed, indicating superparamagnetic property.[45] The saturation magnetization of PVC5Fe is 11.5 emu/g, PVC3G5Fe and PVC5G5Fe are 11.7 emu/g and 12.0 emu/g, respectively. The decrease in saturation magnetization of PVC/Fe_3O_4 composites when compared with Fe_3O_4 nanoparticles is ascribed to the presence of polymer and some ingredients. The superparamagnetic properties of the composites further confirm that the oxide is Fe_3O_4 rather than γ-Fe_2O_3 (supported by the XPS spectra for Fe 2p).

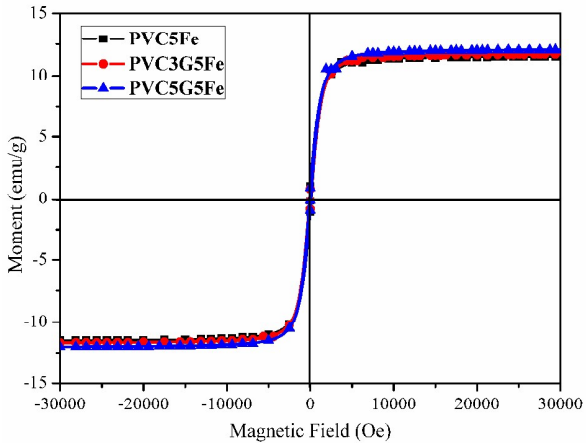

Fig. 10 M–H loops of PVCxGyFe.

3.6 Electrical conductivity

Generally, improved dispersion of graphene is helpful for their formation of a conducting network in polymer matrix.[46] Besides, owing to the advantage of the dispersion method used in this work, we expect that it can bring us a surprised electrical conductivity. As we see from Fig. 11, PVC3G and PVC5G composites are much less conductive than PVC3G5Fe and PVC5G5Fe nanocomposites. With 5 wt% of graphene, the PVC composite is less conductive with a low conductivity of 1.1×10^{-9} S/m. This can be ascribed to poor dispersion of graphene in PVC matrix. Compared to PVC/graphene composites, PVCxGyFe counterparts exhibit greatly improved conductivity. With 5 wt% of graphene and 5 wt% of Fe_3O_4 nanoparticles, the conductivity approaches to 7.7×10^{-4} S/m. The different performances of PVCxG and PVCxGyFe clearly indicate the importance of improved dispersion of conducting fillers in improving conductivity of polymers.

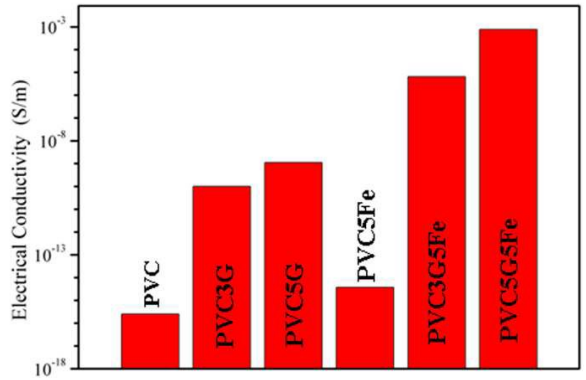

Fig. 11 Plots of electrical conductivity for PVC composites

3.7 EMI shielding

EMI shielding materials are important for modern computer and telecommunication technologies; ranging from commercial and scientific electronic instruments to antenna systems and military electronic devices. Considerable attention has been paid in recent years to the development of EMI shielding materials for potential applications.[47-48] The above-mentioned hybrid materials, consisting of graphene, magnetic nanocrystals and polymers, exhibit multifunctional properties such as superparamagnetic behavior, good electrical conductivity and mechanical properties. The materials with both electrical and magnetic properties are very attractive to the applications of electro-magnetic devices. Here we demonstrate that these multifunctional hybrid composites are potential as electromagnetic interference (EMI) shielding materials.

In this study, the EMI SE (shielding effectiveness) of samples with a thickness of 1.8 mm was measured in X-band (8−12 GHz). Fig. 11a shows the EMI shielding curves of PVC and PVC composites. The pure PVC exhibits hardly any EMI SE in the X-band frequency region (8-12GHz) because of its insulating character. Due to the superparamagnetic properties, PVC5Fe exhibited a microwave absorbing intensity with 2.5 dB. The EMI SE of the composites with 3 wt % and 5 wt % graphene are measured to be 3.7 and 3.8 dB over the frequency range of 8−12 GHz. Compared to pure PVC, the addition of only graphene does not show obvious improvement in EMI SE, which is attributed to poor dispersion states of graphene. However, very strikingly, the ternary composites shows a remarkable effect, up to almost 13 dB at loading of 5 wt% graphene and 5 wt% Fe_3O_4 nanoparticles, which is mainly attributed to the formation of conducting interconnected graphene-based sheet networks in the insulating PVC matrix and the magnetic properties. As the EMI performance usually increases with increasing the material thickness, we have reason to believe that the EMI SE value for our PVC composites can be improved to reach the target value (~20 dB) required for practical application by slightly increasing the thickness of specimen.[49]

The relation between transmittance (T), reflectance (R), and absorbance (A) through shielding material is described as T+R+A=1. The SE_{total} is the summation of the SE due to absorption (SE_A), reflection (SE_R), and multiple reflection (SE_M), *i.e.*, $SE_{total}=SE_A+SE_R+SE_M$. The transmittance T is measured from the ratio of P_T (transmitted electromagnetic power) to P_I (incident electromagnetic power), *i.e.*, $T=(P_T/P_I)=(E_T/E_I)^2$. Thus, the SE_{total} of shielding material can be written as $SE_{total}=20\log(E_I/E_T)=-10\log T$. Considering the effective absorbance (A_{eff}), which is defined as $A_{eff}=(1-R-T)/(1-R)$ with respect to the power of the incident EM wave inside the shielding material, the SE due to reflectance and effective absorbance can be described as $SE_R= -10\log(1-R)$ and $SE_A= -10\log[T/(1-R)]$.[50] Fig. 11b demonstrates SE_R for raw and PVC composites. The contribution of reflection to the total EMI SE is larger than the absorption for the systems, because of conductivity of the composites. The results suggest that the resultant materials are promising EMI reflection materials in microwave frequency ranges.

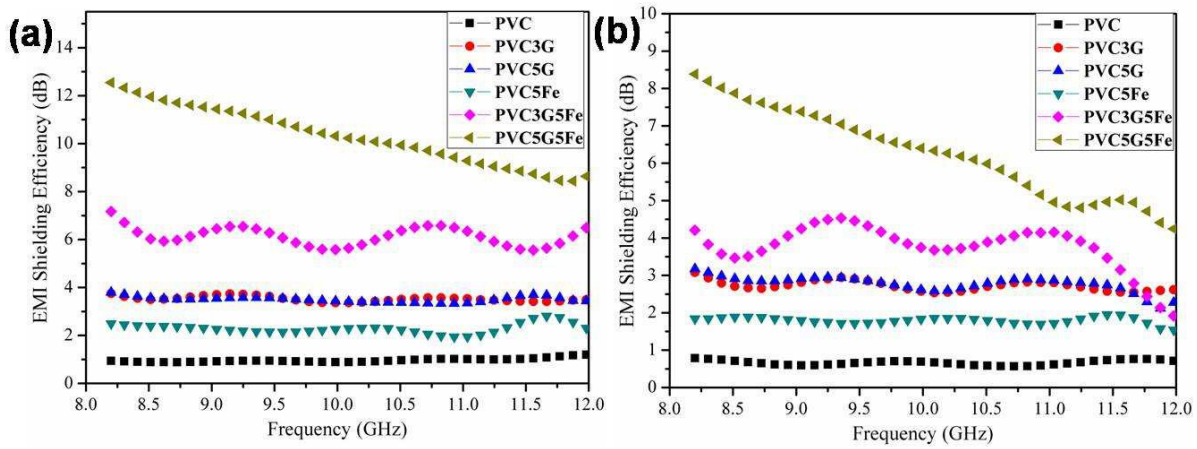

Fig. 12 EMI shielding efficiency as a function of frequency measured in the 8.2-12.4 GHz range of PVC and PVC composites. (a) Total EMI SE (SE_{total}); (b) Microwave reflection (SE_R).

Conclusions

The multifunctional PVC composites were prepared by adding both graphene and Fe_3O_4 nanoparticles into PVC matrix. Owing to ligand exchange, the dispersion of graphene in the PVC was improved with the help of Fe_3O_4 nanoparticles. As a result, the combination between graphene with Fe_3O_4 nanoparticles greatly improved the flame retardancy and smoke suppression of PVC. The presence of well dispersed graphene could build a compact and continuous protective layer with the residual char from PVC degradation on the sample surface during combustion. This not only reduced the release of flammable degradation products, but also acted as an insulating barrier to prohibit the oxygen and feedback of heat from reaching the underlying substrate. In addition, the simultaneous presence of graphene and Fe_3O_4 nanoparticles showed a good reinforcing effect, up to 20.8% increase in tensile strength and 73.7% increase in Young's modulus compared with those of pure PVC. Owing to good dispersion of the nanofiller, the ternary composites showed improved conductivity (7.7×10^{-4} S/m) and electromagnetic shielding efficiency (13 dB) in the X-band frequency region (8-12GHz). It is believed that optimizing the composition between graphene and Fe_3O_4 nanoparticles will further improve the electromagnetic shielding efficiency.

Acknowledgements

This work is financially supported by the National Natural Science Foundation of China for the Projects (51233005 and 51073149), the Ministry of Science and Technology of China (2015AA033901).

Notes and references

[a] *State Key Laboratory of Polymer Physics and Chemistry, Changchun Institute of Applied Chemistry, Chinese Academy of Sciences, Changchun 130022, China. E-mail: ttang@ciac.ac.cn; jiangzw@ciac.ac.cn; Fax: +86 431 85262827; Tel: +86 431 85262004*

[b] *University of the Chinese Academy of Sciences, Beijing 100039, China.*

[c] *Alan G. MacDiarmid Institute, College of Chemistry, Jilin University, Changchun 130012, PR China*

1. Y. Saeki, T. Emura, *Prog. Polym. Sci.*, 2002, **27**, 2055-2131.
2. K. Yao, J. Gong, J. Zheng, L. Wang, H. Tan, G. Zhang, Y. Lin, H. Na, X. Chen, X. Wen, T. Tang, *J. Phys. Chem. C* 2013, **117**, 17016-17023.
3. A. Carretero-Genevrier, C. Boissiere, L. Nicole, D. Grosso, *J. Am. Chem. Soc.*, 2012, **134**, 10761-10764.
4. P. Carty, E. Metcalfe, S. White, *Polymer*, 1992, **33**, 2704-2708.
5. C. Tian, H. Wang, X. Liu, Z. Ma, H. Guo, J. Xu, *J. Appl. Polym. Sci.*, 2003, **89**, 3137-3142.
6. B. Li, *Polym. Degrad. Stab.*, 2002, **78**, 349-356.
7. C. M. Tian, H. Q. Qu, W. H. Wu, H. Z. Guo, J. Z. Xu, *J. Fire Sci.*, 2004, **22**, 41-51.
8. C. Tian, H. Qu, W. Wu, H. Guo, J. Xu, *J. Vinyl Addit. Techn.*, 2005, **11**, 70-75.
9. S. V. Levchik, E. D. Weil, *Polym. Adv. Technol.*, 2005, **16**, 707-716.
10. B. Li, *Polym. Degrad. Stab.*, 2000, **68**, 197-204.
11. X. Wang,; Q. Zhang, *Polym. Int.*, 2004, **53**, 698-707.
12. G. Huang, J. Yang,; J. Gao, X. Wang, *Ind. Eng. Chem. Res.*, 2012, **51**, 12355-12366.
13. P. Kiliaris,; C. D. Papaspyrides, *Prog. Polym. Sci.*, 2010, **35**, 902-958.
14. G. Beyer, *Polym. Adv. Technol.*, 2008, **19**, 485-488.
15. Z. Yang,; B. Li,; F. Tang, *J. Vinyl Addit. Techn.*, 2007, **13**, 31-39.
16. W. Fan, C. Zhang, W. W. Tjiu, K. P. Pramoda, C. B. He, T. X. Liu, *ACS Appl. Mater. Interfaces*, 2013, **5**, 3382-3391.
17. M. Raheel, K. Yao, J. Gong, X. Chen, D. Liu, Y. Lin, D. Cui, M. Siddiq, T. Tang, *Chin. J. Polym. Sci.*, 2015, **33**, 329-338.
18. H. Kim,; A. A. Abdala, C. W. Macosko, *Macromolecules*, 2010, **43**, 6515-6530.
19. J. R. Potts, D. R. Dreyer, C. W. Bielawski, R. S. Ruoff, *Polymer*, 2011, **52**, 5-25.
20. R. Verdejo, M. M. Bernal, L. J. Romasanta, M. A. Lopez-Manchado, *J. Mater. Chem.*, 2011, **21**, 3301-3310.
21. L. Xu, H. Yan, L. Gong, B. Yin, M. Yang, *RSC Adv.*, 2015, **5**, 4238-4244.
22. X. Qian, L. Song, B. Yu, B. Wang, B. Yuan, Y. Shi, Y. Hu, R. K. K. Yuen, *J. Mater. Chem. A*, 2013, **1**, 6822-6830.
23. J. Tang, S. Li, Y. Wang, T. Tang, *Chin. J. Polym. Sci.*, 2013, **31**, 1329-1333.
24. T. Ramanathan; A. A. Abdala, S. Stankovich, D. A. Dikin, M. Herrera Alonso, R. D. Piner, D. H. Adamson, H. C. Schniepp, X. Chen; R. S. Ruoff, S. T. Nguyen, I. A. Aksay, R. K. Prud'Homme, L. C. Brinson, *Nat. Nano*, 2008, **3**, 327-331.
25. K. Yao, H. Tan, Y. Lin, G. Zhang, J. Gong, J. Qiu, T. Tang, H. Na, Z. Jiang, *RSC Adv.*, 2014, **4**, 64053-64060.
26. X. Qi, K. Y. Pu, H. Li, X. Zhou, S. Wu, Q. L. Fan, B. Liu, F. Boey, W. Huang, H. Zhang, *Angew. Chem. Int. Ed.*, 2010, **49**, 9426-9429.
27. Y. Liang, D. Wu, X. Feng, K. Müllen, *Adv. Mater.*, 2009, **21**, 1679-1683.
28. M. Lotya, Y. Hernandez, P. J. King, R. J. Smith, V. Nicolosi, L. S. Karlsson, F. M. Blighe, S. De, Z. Wang, I. T. McGovern, G. S. Duesberg, J. N. Coleman, *J. Am. Chem. Soc.*, 2009, **131**, 3611-3620.
29. K. Yao,; G. Zhang, Y. Lin, J. Gong, H. Na, T. Tang, *Polym. Chem.*, 2014, **6**, 389-396.
30. M. Fang, K. Wang, H. Lu, Yang, Y.; S. Nutt, *J. Mater. Chem.*, 2010, **20**, 1982-1992.
31. H. J. Salavagione, G. Martinez, *Macromolecules*, 2011, **44**, 2685-2692.
32. S. Vadukumpully, J. Paul, N. Mahanta, S. Valiyaveettil, *Carbon*, 2011, **49**, 198-205.
33. D. C. Marcano, D. V. Kosynkin, J. M. Berlin, A. Sinitskii,; Z. Sun, A. Slesarev, L. B. Alemany, W. Lu, J. M. Tour, *ACS Nano*, 2010, **4**, 4806-4814.
34. H. C. Schniepp, J. Li, M. J. McAllister, H. Sai, M. Herrera-Alonso, D. H. Adamson, R. K. Prud'homme, R. Car, D. A. Saville, I. A. Aksay, *J. Phys. Chem. B*, 2006, **110**, 8535-8539.
35. L. Cui, H. Xu, P. He, K. Sumitomo, Y. Yamaguchi, H. Gu, *J. Polym. Sci. Part A: Polym. Chem.*, 2007, **45**, 5285-5295.
36. S. K. Brauman, *J. Fire Retar. Chem.*, 1980, **7**, 119-129.
37. J. Gong, K. Yao, J. Liu, Z. Jiang, X. Chen, X. Wen, E. Mijowska, N. Tian, T. Tang, *J. Mater. Chem. A*, 2013, **1**, 5247-5255.
38. D. Kong, H. Yang, Y. Yang, S. Wei, J. Wang, B. Cheng, *Mater. Lett.*, 2004, **58**, 3503-3508.
39. N. Tian, J. Gong, X. Wen, K. Yao, T. Tang, *RSC Adv.*, 2014, **4**, 17607-17614.
40. T. Karayildirim, J. Yanik, M. Yuksel, M. Saglam, C. Vasile, H. Bockhorn, *J. Anal. Appl. Pyrolysis*, 2006, **75**, 112-119.
41. G. Sivalingam, R. Karthik, G. Madras, *Ind. Eng. Chem. Res.*, 2003, **42**, 3647-3653.
42. T. Kashiwagi, F. Du, J. F. Douglas, K. I. Winey, R. H. Harris, J. R. Shields, *Nat. mater.*, 2005, **4**, 928-933.
43. B. Dittrich, K. A. Wartig, D. Hofmann, R. Mülhaupt, B. Schartel, *Polym. Degrad. Stab.*, 2013, **98**, 1495-1505.
44. J. Liang, Y. Huang, L. Zhang, Y. Wang, Y. Ma, T. Guo, Y. Chen, *Adv. Funct. Mater.*, 2009, **19**, 2297-2302.
45. D. Kechrakos, K. N. Trohidou, *J. Magn. Magn. Mater.*, 2003, **262**, 107-110.
46. W. Li,; X. Z. Tang, H. B. Zhang, Z. G. Jiang, Z. Z. Yu, X. S.Du, Y. W. Mai, *Carbon*, 2011, **49**, 4724-4730.
47. C. T. Lin, B. Swanson, M. Kolody, C. Sizemore, J. Bahns, *Prog. Org. Coat.*, 2003, **47**, 190-197.
48. K. Hayashida, Y. Matsuoka, Carbon, 2015, doi:10.1016/j.carbon.2015.01.006
49. S. Maiti, N. K. Shrivastava, S. Suin, B. B. Khatua, *ACS Appl. Mater. Interfaces*, 2013, **5**, 4712-24.
50. Y. Chen, Y. Wang, H. B. Zhang, X. Li, C. X. Gui, Z. Z. Yu, *Carbon*, 2015, **82**, 67-76.

For Table of Contents only

Flammability properties and electromagnetic interference shielding of PVC/graphene composites containing Fe_3O_4 nanoparticles

Kun Yao [a, b], Jiang Gong [a, b], Nana Tian [a], Yichao Lin [a, b], Xin Wen [a], Zhiwei Jiang [a*], Hui Na [c] and Tao Tang [a,*]

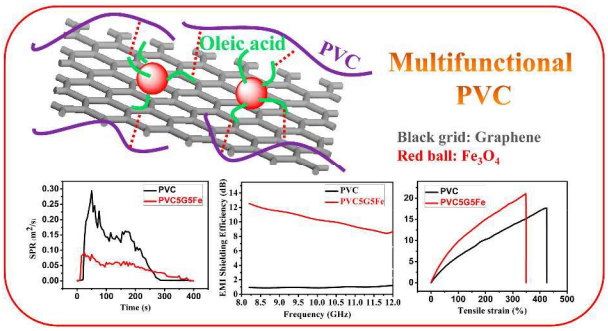

The presence of combined graphene with Fe_3O_4 nanoparticles in PVC matrix can endow the resulting nanocomposites with improved flame retardancy and electromagnetic interference shielding properties besides reinforced mechanical properties.